X-ray and spectroscopic investigations of the structure of yttrium acetate tetrahydrate

F. Ribot, P. Toledano and **C. Sanchez***

Chimie de la Matière Condensée (URA 302), Tour 54 — 5ème étage, Université Pierre et Marie Curie, 4 place Jussieu, 75252 Paris Cédex 05 (France)

(Received December 14, 1990; revised March 18, 1991)

Abstract

The molecular structure of $Y(CH_3CO_2)_3 \cdot 4H_2O$ has been determined by X-ray diffraction. The crystals are triclinic with space group $P\bar{1}$ ($a = 8.867$, $b = 9.368$, $c = 10.587$ Å, $\alpha = 90.30$, $\beta = 115.65$, $\gamma = 119.11°$). The molecule has a dimeric structure where the yttrium atoms have a ninefold coordination. Yttrium atoms are linked by two chelating bridging (polymeric) acetates. Each metal coordination sphere is completed by two other chelating acetate groups and two water molecules. The title compound and other hydrated rare earth acetates which exhibit different structures (lanthanum, praseodymium and neodymium) have also been investigated by IR and ^{13}C CP-MAS NMR spectroscopies. A correlation between spectroscopic data and coordination mode of the carboxylate groups in rare earth acetates is proposed.

Introduction

The so-called 'sol–gel' process offers new approaches to the synthesis of inorganic materials [1]. Molecular precursors lead to the formation of a solid network through hydrolysis and polycondensation reactions. Temperature required for material processing can be noticeably lowered [2]. The molecular precursors are usually inorganic salts or metal alkoxides [3]. They can be chemically modified by chelating ligands such as organic acids or β-diketones [4, 5]. These chemical modifications differentiate hydrolysis reactions and slow down gelation giving rise to a better control of the process [6]. The so-obtained gels are usually amorphous and therefore characterization of their local structure is generally very delicate. Crystalline compounds are very good models to correlate spectroscopic data (IR, NMR, EXAFS, XANES) with structural informations that can be then translated to amorphous materials.

Crystal growth inside gels is also a well known technique where non-stoichiometry, convection currents, turbulence and lattice disruptions due to pronounced thermal vibrations can be prevented. Contamination by impurities and crystalline imperfections can thus be minimized [7]. Complexation of yttrium by acetic acid in aqueous solution gives rise to interesting properties such as the ability to obtain a gel through addition of aqueous ammonia. Large single crystals of hydrated yttrium acetate can be grown from these gels.

This paper reports a structural characterization of $Y(CH_3CO_2)_3 \cdot H_2O$ by X-ray diffraction, IR and ^{13}C CP MAS NMR spectroscopies. The thermal evolution of yttrium acetate tetrahydrate into yttrium sesquioxide has also been investigated. Spectroscopic investigations have been extended to two other families of hydrated rare earth acetates. The first one is composed of lanthanum and cerium acetates, the second one of praseodymium and neodymium acetates. Correlations between spectroscopic data and coordination mode of acetate ligands in rare earth carboxylates are proposed.

Experimental

Synthesis

Yttrium triacetate tetrahydrate ($Y(CH_3CO_2)_3 \cdot 4H_2O$) single crystals were prepared by the gel route. The gel was synthesized by neutralizing a 2 M solution of yttrium nitrate in acetic acid with ammonia (11 M), with the following experimental conditions: $[CH_3CO_2H]/[Y^{3+}] = 2$ and $[NH_4OH]/[Y^{3+}] = 4$. After neutralization, the mixture was deposited onto a glass substrate, and gelation occurred within about 4 h.

*Author to whom correspondence should be addressed.

0020-1693/91/$3.50

© 1991 — Elsevier Sequoia, Lausanne

Single crystals of 5 mm^3 grew up from this gel in about 15 days. These crystals were then removed and quickly washed with distilled water. Elemental analysis of the crystalline compound was carried out. Found: Y, 23.9; C, 21.3; H, 5.0; Calc. for $Y(CH_3CO_2)_3 \cdot 4H_2O$: Y, 26.3; C, 21.3; H, 5.0%. The deuterated compound $Y(CD_3CO_2)_3 \cdot 4D_2O$ was prepared by dissolution under argon of yttrium oxide in a 50% solution of deuterated acetic acid in D_2O, in order to prepare a 1 M yttrium solution. After refluxing for 2 h, the solution was evaporated under vacuum. The deuterated solid was then washed with D_2O and filtered [8]. Lanthanum, praseodymium and neodymium acetates were prepared by adding stoichiometric amounts ($CH_3CO_2^-/M^{3+} = 3$) of sodium acetate to an aqueous molar solution of the rare earth nitrates. The precipitate obtained was then filtered and washed with small amounts of distilled water. The crystalline powders were dried in air at 50 °C during 4 h. Chemical analysis correspond to $Nd(CH_3CO_2)_3 \cdot 1.5H_2O$, $Pr(CH_3CO_2)_3 \cdot H_2O$ or $La(CH_3CO_2)_3 \cdot H_2O$.

Characterization

TGA and DSC experiments were simultaneously performed on a NETZSCH thermal analyser STA 409 under a static air atmosphere. The final temperature was 900 °C with a heating rate of 5°/min. IR spectra were recorded on a Perkin-Elmer 783 spectrometer, equipped with a home made high temperature cell (maximum 300 °C). The frequency range was 4000–400 cm^{-1}. The samples were studied as powders dispersed in KBr pellets. ^{13}C NMR spectra were obtained at room temperature in the solid state by proton enhanced NMR on a Brucker CXP300 operating at 300.13 MHz for protons and 75.4 MHz for carbon. MAS spectra were obtained at spinning speeds up to 4000 Hz.

Crystal structure and refinement

The crystal structure was determined by single crystal X-ray diffraction. Intensity data were collected on a Philips PW1100 diffractometer equipped with a graphite monochromator. Unit cell parameters were refined from the powder diffraction pattern (63 reflections with $4.8° < \theta < 26°$). Crystal data, data collection parameters, and residual from refinement are summarized in Table 1. During the intensity data collection, three standard reflections, $\bar{2}\,\bar{2}\,0$, $2\,2\,0$ and $\bar{1}\,\bar{7}\,0$ were measured every 2 h and showed less than 2% variation in intensity. Background was measured before and after every scan. Intensities were corrected for Lorentz and polarization factors. No absorption corrections were applied. Atomic scattering factors including anomalous terms were taken from the International Tables for X-Ray Crystallography (1974). Direct methods (MULTAN78 [9]) and difference Fourier calculations were used for structure solution. Refinements were made by full-matrix least-squares (SHELX76 [9]) with anisotropic temperature factors for the 17 atoms other than hydrogen. The 17 hydrogen positions were calculated by SHELX76 assuming rigid groups (CH_3 or OH_2). For methyl groups, the C–CH_3 rotation angle was refined. Hydrogen positions were used in structure factor calculations without any further refinement. Final non-weighted residual factor, R, was equal to 0.046 (maximal shift/error $\Delta/\sigma = 0.4$). Maximum height in final difference map: two peaks of 1.2 e $Å^{-3}$ around Y atom (less than 1 Å).

TABLE 1. Crystallographic data for $Y_2(\mu_2\text{-}CH_3CO_2)_2(CH_3CO_2)_4(H_2O)_4 \cdot 4H_2O$

Formula	$Y_2(CH_3CO_2)_6(H_2O)_4 \cdot 4H_2O$
Molecular weight	676.20
a (Å)	8.867(1)
b (Å)	9.368(2)
c (Å)	10.587(2)
α (°)	90.30(2)
β (°)	115.65(1)
γ (°)	119.11(1)
V ($Å^3$)	666.1(3)
Space group, Z	$P\bar{1}$, 1
Crystal size (mm)	$0.20 \times 0.15 \times 0.15$
Density (g cm^{-3})	1.69
Scan mode	$\omega/2\theta$
Radiation	λ(Mo Kα) = 0.71069 Å
μ (cm^{-1})	45.6
$F(000)$	344
Temperature (°C)	25
θ_{max} (°)	26
hkl_{max}	9 11 12
θ scan rate (°s^{-1})	0.01
θ scan length	$1.2 + 0.3°\text{tg}\theta$
No. unique reflections measured	2199
No. reflections observed	1935 $I > 3\sigma(I)$
$R = [\Sigma \|\|F_o\| - \|F_c\|\|]/\Sigma\|F_o\|$	0.046
$R_w = [\Sigma w(\|F_o\| - \|F_c\|)^2 / \Sigma w\|F_o\|^2]^{1/2}$ $w = 1$	0.052

Results and discussion

X-ray structure of $Y(CH_3CO_2)_3 \cdot 4H_2O$

Atomic positional parameters and equivalent isotropic thermal parameters are listed in Table 2. The main interatomic distances and angles are shown in Table 3. See also 'Supplementary material'. The ORTEP [10] drawing computed with 50% probability thermal ellipsoids of $Y(CH_3CO_2)_3 \cdot 4H_2O$ is shown

TABLE 2. Atomic positional parameters and equivalent isotropic thermal parameters for non-hydrogen atoms in $Y(CH_3CO_2)_3 \cdot 4H_2O$

Atom	x/a	y/b	z/c	B_{eq} (Å^2)
Y	0.6856(1)	0.5967(1)	0.4106(1)	2.27(1)
O1a	0.4392(6)	0.3219(6)	0.2334(5)	4.0(2)
O2a	0.3715(5)	0.3522(5)	0.4018(4)	2.8(2)
O1b	0.4264(6)	0.6530(5)	0.2904(5)	3.3(2)
O2b	0.7321(6)	0.8756(5)	0.4064(5)	3.4(2)
O1c	0.7040(7)	0.6517(6)	0.1969(5)	4.8(2)
O2c	0.8643(6)	0.5379(6)	0.3158(5)	4.3(2)
C1a	0.3257(8)	0.2588(7)	0.2879(6)	2.9(2)
C2a	0.143(1)	0.087(1)	0.217(1)	4.3(3)
C1b	0.5472(9)	0.8139(8)	0.3326(7)	3.4(3)
C2b	0.469(1)	0.927(1)	0.296(1)	6.0(4)
C1c	0.8093(8)	0.5909(7)	0.2091(7)	3.1(3)
C2c	0.862(1)	0.585(1)	0.092(1)	4.9(3)
Ow1	0.7862(6)	0.4457(6)	0.5638(5)	3.9(2)
Ow2	1.0188(6)	0.7972(5)	0.5794(5)	3.6(2)
Ow3	0.5812(7)	0.8206(6)	0.0047(5)	4.6(2)
Ow4	0.7737(8)	0.1695(7)	0.1287(6)	5.4(3)

TABLE 3. Main interatomic distances (Å) and angles (°) for $Y(CH_3CO_2)_3 \cdot 4H_2O$

Y–O1a	2.418(4)	Y–O1c	2.379(6)
Y–O2a(i)	2.351(5)	Y–O2c	2.458(7)
Y–O2a	2.565(4)	Y–Ow1	2.330(6)
Y–O1b	2.415(6)	Y–Ow2	2.334(3)
Y–O2b	2.443(5)	Y–Y(i)	4.163(2)
O2a(i)–Y–O2a		64.3 (1)	
O1a–C1a–O2a		117.3 (4)	
O1b–C1b–O2b		119.2 (8)	
O1c–C1c–O2c		119.0 (8)	

Symmetry code: (i) $1-x$, $1-y$, $1-z$.

in Fig. 1. The molecule has a dimeric structure built with two yttrium atoms in ninefold coordination. The metal atoms are linked by two chelating-bridging (polymeric) acetates. The coordination of the yttrium atom is completed by two other chelating acetate groups and two water molecules. The last two water molecules correspond to water of crystallization. This dimeric unit is similar to the one found for $Er(CH_3CO_2)_3 \cdot 4H_2O$ in a previous structural determination with photographic recordings and isotropic temperature factors ($R = 10.6\%$) [11].

Thermal treatments

TGA and DSC experiments are shown in Fig. 2. The weight loss during the TGA experiment clearly indicates a four step thermal decomposition mechanism which leads to amorphous yttrium sesquioxide. According to the literature [12], the following scheme can be proposed:

$$Y(CH_3CO_2)_3 \cdot 4H_2O \xrightarrow{115\ ^\circ C} Y(CH_3CO_2) \cdot 0.5H_2O + 3.5H_2O$$

$$Y(CH_3CO_2)_3 \cdot 0.5H_2O \xrightarrow{160\ ^\circ C} Y(CH_3CO_2)_3 + 0.5H_2O$$

$$Y(CH_3CO_2)_3 \xrightarrow{380\ ^\circ C} 0.5(Y_2O_2CO_3) + CO_2 + 1.5CH_3COCH_3$$

$$Y_2O_2CO_3 \xrightarrow{590\ ^\circ C} Y_2O_3 + CO_2$$

Water molecules are lost in two stages at 115 and 160 °C to form anhydrous yttrium acetate $Y(CH_3CO_2)_3$. This compound was characterized by IR and its X-ray powder pattern. It is isomorphous with anhydrous erbium acetate previously described [13]. The anhydrous yttrium acetate decomposes into yttrium sesquioxide through the oxycarbonate. The formation of oxycarbonate above 360 °C was checked by IR [12]. Amorphous yttrium sesquioxide, crystallizes above 600 °C into Y_3O_3 type C as confirmed by powder X-ray diffraction [14]. The DSC curve exhibits four endothermic peaks located at 115, 160, 195 and around 390 °C. The last one is overlapped by a strong exothermic peak at 400 °C.The first two peaks can be attributed to the water departure observed in the TGA. The exothermic peak at 400 °C appears at higher temperature than the maximum slope of the TGA. It can be correlated with the combustion, above the sample, of organic species evolved from the anhydrous acetate during its transformation into oxycarbonate as was indicated by the endothermic take off. The third peak (195 °C) always appears after scanning the temperature up and down between room temperature and 250 °C. An accurate interpretation of this peak would be difficult. It was previously attributed to a transition between polymeric acetates and monodentate acetates on the basis of DTA and low frequency IR data [15]. IR spectra of the yttrium acetate hydrate were recorded in the r.t. to 250 °C temperature range. Throughout the thermal treatment the characteristic features of monodentate acetate groups [16] ($\nu_{as} \approx 1700$, $\nu_s \approx 1300$ and $\Delta\nu = 400$–450 cm^{-1}) do not appear. At the end of the thermal treatment, the characteristic features of polymeric or chelating acetate groups only are observed ($\nu_{as}(COO^-) = 1555$, $\nu_s(COO^-) = 1450$ and $\Delta\nu = 105$ cm^{-1}). Consequently, the third DSC endothermic peak should be due to transitions involving only polydentate acetate groups.

Infrared

The IR spectrum of $Y(CH_3CO_2)_3 \cdot 4H_2O$ is shown in Fig. 3. IR bands are reported in Table 4. This spectrum can be divided into three distinctive regions.

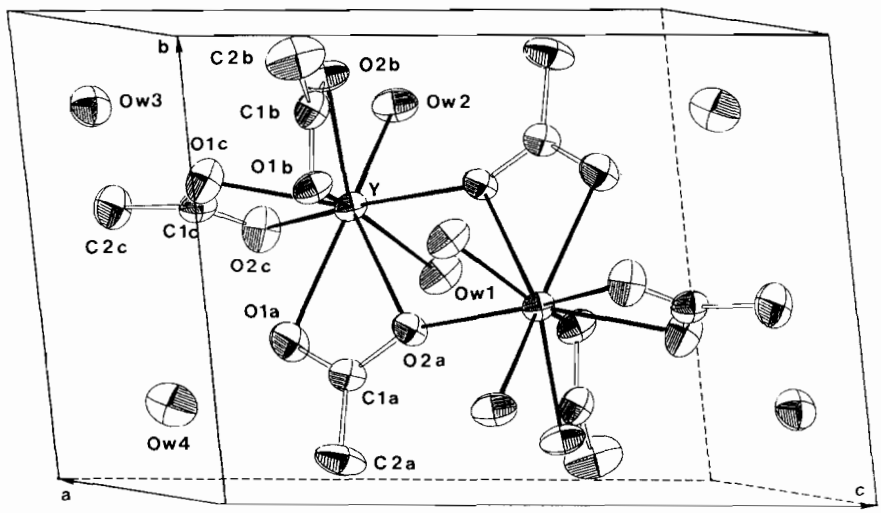

Fig. 1. ORTEP drawing of $Y_2(\mu_2\text{-}CH_3CO_2)_2(CH_3CO_2)_4(H_2O)_4 \cdot 4H_2O$.

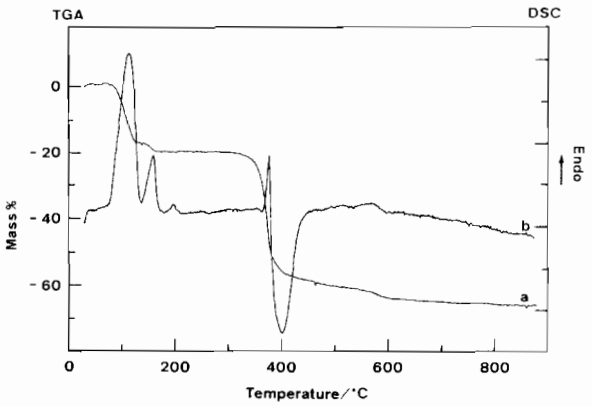

Fig. 2. TGA (a) and DSC (b) for $Y(CH_3CO_2)_3 \cdot 4H_2O$.

High energy bands, around 3400 and 2935 cm^{-1} correspond to ν(O–H) and ν(C–H) stretching vibrations, respectively. On the low energy side of the spectrum, three sets of bands appear, corresponding to rocking $\rho(CH_3)$ (around 1000 cm^{-1}), stretching ν(C–C) (around 950 cm^{-1}) and deformation $\delta(COO^-)$ (between 450 and 700 cm^{-1}) vibrations, respectively. On the middle energy range, three sets of bands (δ(OH), ν(COO), $\delta(CH_3)$) contribute to the IR spectrum. One set located at 1700 and 1660 cm^{-1} correspond to deformation mode δ(O–H) of the water molecule. Another set is the characteristic strong band of acetate ligands appearing around 1500 cm^{-1}.

Four kinds of coordination of acetate groups are generally considered, according to the literature [16]: monodentate(I), chelating(II), bridging(III) and polymeric(IV). They are schematically represented in Fig. 4. They are characterized by the position and

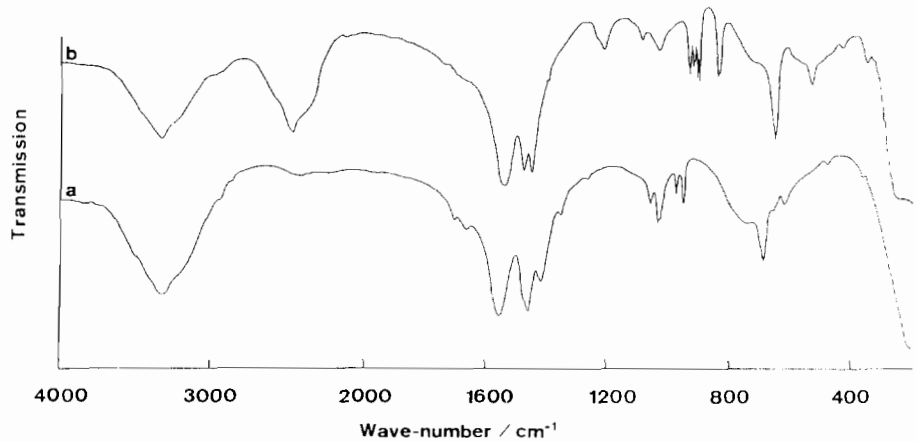

Fig. 3. IR spectra of $Y(CH_3CO_2)_3 \cdot 4H_2O$ (a) and $Y(CD_3CO_2)_3 \cdot 4xD_2O \cdot xH_2O$ (b).

TABLE 4. IR bands of $Y(CH_3CO_2)_3 \cdot 4H_2O$

$\nu(cm^{-1})$	Assignment	$\nu(cm^{-1})$	Assignment	$\nu(cm^{-1})$	Assignment
3310b	ν(OH)	1460s	$\nu_s(CO_2^-)$	965m	ν_{as}(CC)
3020sh	ν_{as}(CH)	1415m	$\delta(CH_3)$	945m	ν_s(CC)
2935w	ν_s(CH)	1350w	$\delta(CH_3)$	680w	$\delta(CO_2^-)$
1700w	δ(OH)	1050m	$\rho(CH_3)$	645w	$\delta(CO_2^-)$
1665w	δ(OH)	1025m	$\rho(CH_3)$	610w	$\rho(CO_2^-)$
1550s	$\nu_{as}(CO_2^-)$	1015sh	$\rho(CH_3)$	455w	$\rho(CO_2^-)$
1475sh	$\nu_s(CO_2^-)$				

s:strong, m: medium, w: weak, b: broad.

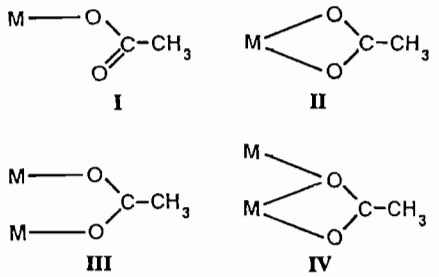

Fig. 4. Schematical representation of the coordination modes for acetate ligand.

the difference between the asymmetric and symmetric vibrations of the carboxylate group. However, in the same region (1400–1500 cm^{-1}), the bending mode $\delta_{as}(CH_3)$ should appear. This gives rise to some disagreements concerning the assignment of the stretching vibrations for acetate groups [8, 13, 16, 17]. Therefore we have performed a deuteration study in order to clarify this assignment. The IR spectra for the deuterated yttrium acetate is shown in Fig. 3. After deuteration, the first important feature observed in the IR spectrum is the disappearance of the band located at 1415 cm^{-1}; thus this band can be attributed to $\delta_{as}(CH_3)$. Bands located at 1550, 1475 and 1460 cm^{-1} in the non-deuterated compound are slightly shifted downward to 1535, 1470 and 1445 cm^{-1}. They can be respectively assigned to $\nu_{as}(COO^-)$ and $\nu_s(COO^-)$ vibrations. The exchange of water, with D_2O, gives rise to a second kind of features. A new set of bands located at 1240 and 1217 cm^{-1} is observed. They can be attributed to δ(O–D) bending modes. They correspond to the δ(O–H) mode shifted under deuteration, which were previously observed at 1700 and 1660 cm^{-1}. At the same time, a new set of bands corresponding to ν(O–D) vibrations is observed around 2500 cm^{-1}. The comparison between deuterated and non-deuterated samples, indicates that all components are shifted under deuteration and their isotropic frequency ratio is about 1.36–137. It also clearly indicates the presence of two kinds of water molecules, in agreement with our X-ray data. One is directly bonded to yttrium, and weakly hydrogen bonded. It is characterized by ν(O–H) = 3450–3420 cm^{-1}, δ(O–H) = 1700 cm^{-1}, ν(O–D) = 2560–2470 cm^{-1}, δ(O–D) = 1240 cm^{-1}. The other one should correspond to crystallization water more strongly hydrogen bonded and characterized by lower vibration frequencies (ν(O–H) = 3300–3200 cm^{-1}, δ(O–H) = 1660 cm^{-1}, ν(O–D) = 410–2370 cm^{-1}, δ(O–D) = 1217 cm^{-1}). For hydrogen bonded water molecules a correlation between IR frequency and oxygen–oxygen distance (O–H–O) was established by Novak [18] and Nakamoto *et al* [19]. Distances (O–H–O) of about 2.7–2.8 Å found from $Y(CH_3CO_2)_3 \cdot 4H_2O$ IR data are in good agreement with the X-ray structure, which exhibits oxygen–oxygen distances ranging between 2.67 and 2.9 Å. Three other rare earth acetates ($La(CH_3CO_2)_3 \cdot H_2O$, $Nd(CH_3CO_2)_3 \cdot 1.5H_2O$ and $Pr(CH_3CO_2)_3 \cdot H_2O$ have been studied by IR absorption. Karraker [13] found three different features for the IR spectra of the hydrated rare earth acetates. One is observed for lanthanum and cerium, one for neodymium and praseodymium, and a final one for elements ranging from samarium to lutetium. As expected from the ionic radius, the IR spectra of hydrated yttrium acetate shows the features of the last series. Single crystal X-ray diffraction studies on cerium [20] and praseodymium [21] hydrated acetates show that both compounds contain bridging and polymeric acetate groups in a 1:2 ratio. On the other hand our work shows that hydrated yttrium acetate which is isostructural to the hydrated acetates from samarium to lutetium [22] contains chelating and polymeric acetate groups in a 2:1 ratio. All the polydentate coordination modes of the acetate group in rare earth complexes are therefore covered by lanthanum, praseodymium and yttrium derivatives. The stretching vibrations of the acetate group and their assignments are listed Table 5. Bridging acetates are clearly characterized by a carboxylate asymmetric stretching vibration at around 1600 cm^{-1} and a $\Delta\nu$ of around 170 cm^{-1}. Chelating and polymeric acetates

TABLE 5. Stretching vibrations (cm^{-1}) and coordination mode of the carboxylate groups in different rare earth hydrated acetates

Compound	$\nu_{as}(CO_2^-)$	$\nu_s(CO_2^-)$	$\Delta\nu$	Coordination mode (quantity)
$La(CH_3CO_2)_3 \cdot H_2O$	1590(sh)	1425	165	bridging (1)
	1560	1450	110	polymeric (2)
$Pr(CH_3CO_2)_3 \cdot H_2O$ and	1605(sh)	1425	180	bridging (1)
$Nd(CH_3CO_2)_3 \cdot 3/2H_2O$	1540	1445	95	polymeric (1)
		1465	75	polymeric (1)
$Y(CH_3CO_2)_3 \cdot 4H_2O$	1550(b)	1460	90	polymeric (1)
		1475	75	chelating (2)

sh: shoulder, b: broad.

are more difficult to differentiate on the basis of IR.

^{13}C CP-MAS

^{13}C NMR has a better resolution for small differences in local structure [23, 24] but the presence of paramagnetic species gives huge effects on the chemical shift [21] and therefore direct correlation is difficult. ^{13}C CP-MAS NMR studies on two diamagnetic hydrated rare earth acetates, lanthanum and yttrium, which exhibit different acetate coordination types were carried out in order to clarify the assignment between polymeric and chelating acetates. The ^{13}C CP-MAS spectrum of the title compound $Y(CH_3CO_2)_3 \cdot 4H_2O$ is shown in Fig. 5. It exhibits two sets of three resonances. The first one around 23 ppm (22.4, 23.0, 23.5) and the second one around 185 ppm (185.2, 188.0, 188.5). They are respectively characteristic of the methyl and carbonyl ^{13}C isotropic chemical shift of an acetate group bonded to a metal atom [25]. The other peaks correspond to the spinning side bands. Correlation between the coordination mode and the isotropic chemical shift can be proposed on the basis of the ratio (1:2) between polymeric and chelating acetates observed in the structure. The resonance around 185 ppm should be attributed to polymeric acetates and resonance around 188 ppm to chelating acetates.

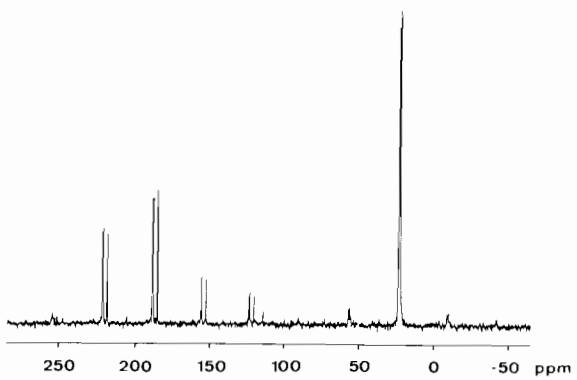

Fig. 5. ^{13}C CP-MAS NMR spectrum of $Y(CH_3CO_2)_3 \cdot 4H_2O$.

The ^{13}C CP-MAS spectrum of $La(CH_3CO_2)_3 \cdot H_2O$ has also been recorded. It also exhibits three different acetate groups characterized by three isotropic chemical shifts of carbonyl located at 188.1, 186.0 and 185.8 ppm and only two resolved methyl ^{13}C resonances at 23.7 and 24.7 ppm. On the basis of the ratio between bridging and polymeric acetates (1:2) and the assignment of the carbonyl chemical shift in yttrium acetate, again the peaks around 186 ppm could be attributed to polymeric acetates and the peak at around 188 ppm to bridging acetate. The O–C–O angle is reported in the literature to play an important role on the isotropic chemical shift [24] or on the stretching vibrations [17] of the carboxylate. For $Y(CH_3CO_2)_3 \cdot 4H_2O$ there is a straightforward relationship between O–C–O angles and isotropic chemical shifts (117.3° → 185.2 ppm, 119.0° → 188.0 ppm, 119.2° → 188.5 ppm). Unfortunately the O–C–O angles for lanthanum acetate were not available to obtain a complete assignment. However, from NMR results, the O–C–O angles in bridging and chelating ligands should be very close.

Conclusions

IR spectroscopy and ^{13}C CP-MAS NMR, when used together, can give clear evidence relating to the coordination mode of carboxylate ligands in rare earth acetates. IR allows differentiation between monodentate and bidentate coordination modes. Moreover a careful analysis of the stretching COO^- vibrations allows one to distinguish separation between bridging and other types of bidentate coordination modes (chelating, polymeric). ^{13}C NMR appears to be more appropriate to differentiate polymeric acetates among the other types.

Supplementary material

All calculated atomic coordinates, anisotropic thermal parameters, bond lengths and angles and a listing of h,k,l, F_o and F_c and powder diffraction pattern are available from the authors on request.

Acknowledgements

We wish to thank Rhône-Poulenc Company for its financial support, and the application laboratory of Bruker France for NMR experiments.

References

1 B. J. J. Zelinsky and D. R. Uhlmann, *J. Phys. Chem. Solids, 45* (1984) 1069.
2 J. D. Mackenzie, *J. Non-Cryst. Solids, 73* (1985) 631.
3 J. Livage, M. Henry and C. Sanchez, *Prog. Solid. State Chem., 18* (1988) 259.
4 C. Sanchez, F. Babonncau, S. Docuff and A. Leaustic, in J. D. Mackenzie and D. R. Ulrich (eds.), *Ultrastructure Processing of Advanced Ceramics,* Wiley, New York, 1988, p. 77.
5 R. C. Mehrotra, R. Bohra and D. P. Gaur, *Metal β-Diketonates and Allied Derivatives,* Academic Press, London, 1978.
6 C. Sanchez, J. Livage, M. Henry and F. Babonneau, *J. Non-Cryst. Solids, 100* (1988) 65.
7 S. K. Arura, *Prog. Crystal Growth Charact., 4* (1981) 345.
8 J. R. Ferraro and M. J. Becker, *J. Inorg. Chem., 32* (1970) 1495.
9 (a) P. Main, S. E. Hull, L. Lessinger, G. Germain, J.-P. Declercq and M. M. Woolfen, *MULTAN 78,* Department of Physics, University of York, York, U.K., 1978; (b) G. M. Sheldrick, *SHELX 76,* University of Cambridge, U.K., 1976.
10 C. K. Johnson, *ORTEP,* Chemistry Division, Oak Ridge National Laboratory, Oak Ridge, TN, U.S.A., 1965.
11 L. A. Aslanov, I. K. Abdul'minev, M. A. Porai-Koshits and V. I. Ivanov, *Dokl. Akad. Nauk SSSR, 205* (1972) 343.
12 K. C. Patil, G. V. Chandrasheckar, M. V. George and C. N. R. Rao, *Can. J. Chem., 46* (1968) 257.
13 D. G. Karraker, *J. Inorg. Nucl. Chem., 31* (1969) 2815.
14 *Powder Diffraction File,* Card No. 5-0574, Joint Committee in Powder Diffraction Standards, Swarthmore, PA, 1981.
15 G. Adachi and E. A. Secco, *Can. J. Chem., 50* (1972) 3100.
16 K. Nakamoto, *Infrared and Raman Spectra of Inorganic and Coordination Compounds,* Wiley, New York, 1978, p. 232.
17 A. I. Grigor'ev and V. N. Maksimov, *Russ. J. Inorg. Chem., 9* (1964) 580.
18 A. Novak, *Struct. Bonding (Berlin), 18* (1974) 177.
19 K. Nakamoto, M. Morgoshes and R. E. Rundle, *J. Am. Chem. Soc., 77* (1955) 6480.
20 G. G. Sadikov, G. A. Kukima and M. A. Porai-Koshits, *Zh. Strukt. Khim., 8* (1967) 531.
21 S. Ganapathy, V. P. Chacko, R. G. Bryant and M. C. Etter, *J. Am. Chem. Soc., 108* (1986) 3159.
22 R. Vadura and Kvapil, *J. Mater. Res. Bull., 6* (1971) 865.
23 R. G. Bryant, V. P. Chacko and M. C. Etter, *Inorg. Chem., 23* (1984) 3580.
24 N. R. Jagannathan, *Chem. Phys. Lett., 140* (1987) 548.
25 R. K. Harris and B. E. Mann, *NMR and Periodic Table,* Academic Press, London, 1978.